IEEE Access
Multidisciplinary | Rapid Review | Open Access Journal

Received February 6, 2017; accepted March 9, 2017, date of publication April 5, 2017, date of current version June 7, 2017.

Digital Object Identifier 10.1109/ACCESS.2017.2691402

Experimental Study of MIMO-OFDM Transmissions at 94 GHz in Indoor Environments

CONCEPCIÓN SANCHIS-BORRÁS[1], MARÍA-TERESA MARTÍNEZ-INGLÉS[2], JOSÉ-MARÍA MOLINA-GARCÍA-PARDO[3], JUAN PASCUAL GARCÍA[3], AND JOSÉ-VÍCTOR RODRÍGUEZ[3]

[1]Department of Technical Sciences, Universidad Católica San Antonio de Murcia, 30107 Murcia, Spain
[2]University Center of Defense, San Javier Air Force Base, Ministerio de Defensa-Universidad Politécnica de Cartagena, 30720 Santiago de la Ribera, Spain
[3]Information Technologies and Communications Department, Universidad Politécnica de Cartagena, Cartagena 30202, Spain

Corresponding author: Concepción Sanchis-Borrás (csanchis@ucam.edu)

This work was supported in part by the Ministerio de Economía y Competitividad MINECO, Spain under Grant TEC2016-78028-C3-2-P, and in part by the European FEDER funds.

ABSTRACT Millimeter wave (mm-wave) frequencies have been proposed to achieve high capacity in 5G communications. Although meaningful research on the channel characteristics has been performed in the 28-, 38-, and 60-GHz bands in both indoor and short-range scenarios, only a small number of trials (experiments) have been carried out in other mm-wave bands. The objective of this paper is to study the viability and evaluate the performance of the 94-GHz frequency band for MIMO-OFDM transmission in an indoor environment. Starting from a measurement campaign, the performance of MIMO algorithms is studied in terms of throughput for four different antenna configurations.

INDEX TERMS MIMO, mm-wave, 94 GHz, OFDM, space time coding.

I. INTRODUCTION

The exploitation of millimeter wave (mm-wave) frequencies for 5G standards has started to gain considerable attention within the wireless industry. There are several reasons for this. Firstly, the amount of mobile traffic data is expected to grow 5000-fold by the year 2030 [1], which, in turn, will require challenging increases in link capacity and spectrum availability. Both requirements can be met by using advanced transmission techniques such as massive Multiple-Input Multiple-Output (MIMO) [2] and also by the extension to the millimeter-wave (mm-wave) bands within the range of 30 – 300 GHz. Secondly, the availability of large blocks of spectrum in this range allows for the trading off of spectral efficiency for bandwidth in the early stages of deployment of this technology.

In this context, various frequency bands have been identified as potentially useful for future wireless networks at the World Radio Conference (WRC'15). Moreover, the first phase of EU's Horizon 2020 5G PPP initiative is investigating the 6 – 100 GHz frequencies, including mm-wave frequencies, for 5G's ultra-high data rate mobile broadband, among other applications.

While significant studies of the channel characteristics are available in the 28, 38, and 60 GHz bands for indoor and outdoor environments [1], only a few trials have been conducted in other mm-wave bands for outdoor and outdoor–indoor environments and scenarios with mobility [3]–[8]. However, mm-wave applications need specific considerations, due to the higher frequencies and wider bandwidths compared to existing standards for 4G Long Term Evolution (LTE) and WLAN below 6 GHz.

More specifically, to the best of the authors' knowledge, little research dealing with propagation and channel modeling in the 94 GHz frequency band has been carried out. Reference [9] presents a preliminary design of a 94 GHz E-band phase array antenna, assuming the existent channel characteristics and configurations of the 60 GHz frequency band [10].

From the point of view of the physical layer (PHY), Orthogonal Frequency Division Multiplexing (OFDM) and MIMO [11] are essential to achieving the throughput and reliability levels projected for 4G and 5G. MIMO techniques have succeeded in increasing the system performance remarkably. Moreover, reliability can be improved by using

antenna diversity, that is, by transmitting multiple copies of the same signal across a number of antennas. Space–time block code (STBC) algorithms combine all the copies of the received signal in an optimal way [12].

Regarding the standardization in mm-wave frequencies, it is worth mentioning the IEEE 802.15.3c for WPAN [13], wireless HD for uncompressed high-definition video streaming, and ECMA-387 standards. For the case of WLAN, two standards are also found: IEEE802.11ad [14] and WiGig (on which IEEE 802.11ad was based), which stretch WLAN into gigabit capabilities through the 60 GHz spectrum. However, for the 94 GHz band, there is not a defined standard because the feasibility of using this band to transmit data at 5G is being investigated.

The aim of this work is to present an experimental study to analyze the viability of wireless communications at 94 GHz. The performance is analyzed in terms of PHY parameters such as the signal-to-noise ratio (SNR), correlation, and the specifications of the IEEE802.15.3c standard. Furthermore, the throughput of different space–time MIMO/OFDM strategies is evaluated, considering different antenna element configurations.

The paper is organized as follows. Section II describes the experimental setting, while Section III presents the characteristics of the channel matrices with regard to SNR and correlation. Section IV analyzes the throughput results for both vertical and horizontal polarization and, finally, section V presents the main conclusions of this work.

FIGURE 1. Laboratory photo.

II. DESCRIPTION OF THE EXPERIMENTAL SETUP

A. Scenario

The scenario for the measurements is a laboratory of the Universidad Politécnica de Cartagena as is shown in Fig.1. The dimensions of the lab are $9.1 \times 4.8 \times 4.1$m, and different cupboards, desks, chairs, and shelves can be found as furniture. The walls are made of plasterboard, and the floor and ceiling are made of concrete.

Fig. 2 depicts the measured scenario as well as the 15 transmitting positions. For the measurements, one position is selected for the receiver (assuming an access point) and is marked as Rx in Fig. 2. For the transmitter, 15 positions are uniformly distributed around the room and marked as 1 to 15. In all the experiments, a line ofsight (LoS) exists.

B. Equipment

The mm-wave channel sounder setup is based on a commercial vector network analyzer, the R&S ZVA 67, and

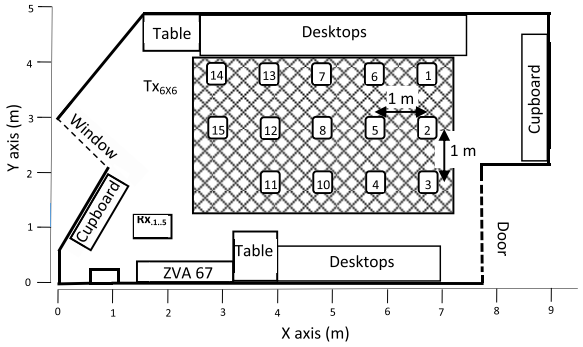

FIGURE 2. Map of the measurements.

TABLE 1. Transmitter system configurations.

Conf1	Conf2	Conf3	Conf4
xooooo	xxxxoo	xoooox	oooooo
xooooo	oooooo	oooooo	oooooo
xooooo	oooooo	oooooo	ooxxoo
xooooo	oooooo	oooooo	ooxxoo
oooooo	oooooo	oooooo	oooooo
oooooo	oooooo	xoooox	oooooo

up-converters as was performed previously in [15]. The R&SZVA-Z110E converter (W-band WR-10, 75 to 110 GHz) was used for both the transmitting and the receiving unit. The system was THROUGH calibrated, with the delay and gain of the antennas being included in the measurements. The measured dynamic range for an intermediate frequency of 10 Hz was 107 dB.

The measured frequency range was 92.5 – 95.5 GHz, using 1024 frequency points. The Rx has a height of 0.784 m, while Tx has a height of 0.886 m. Both in Tx and Rx, two identical polarimetric omni-directional antennas manufactured by Mi-Wave (WR-10) were selected, with a gain of 2dB and an aperture of 30ř in the vertical plane. In each position, the Tx and Rx antennas are moved virtually using a Uniform Rectangular Array (URA) and a Uniform Linear Array (ULA), respectively. For the ULA, five elements were equally spaced, 1 mm apart (0.4λ at 94 GHz), along the Y direction, while for the URA, measurements were performed over a 6×6 uniform rectangular grid with 1 mm spacing along the X and Y directions. Furthermore, two polarization combination measurements were performed, either horizontal Tx and horizontal Rx (HH) or vertical Tx and vertical Rx (VV).

C. CONFIGURATIONS

From the transmitting 6×6 MIMO array, four configurations for the transmitter have been studied, selecting four antennas from the 36 positions.

Table 1 shows the four antenna configurations (Conf1, Conf2, Conf3 and Conf4) considered. It shows the orientation of the four chosen Tx antennas, marked with x's. Moreover, the row and column in each configuration have the same orientation that the y and x axes in Fig. 2, respectively.

So, Conf1 and Conf2 have vertical and horizontal orientations, respectively, while Conf3 and Conf4 have four antennas forming a square, maximizing and minimizing the distance respectively. For Conf3, the distance is six antenna elements while, for Conf4, it is one antenna element. In the receiver, four of the five antennas have been selected with the same orientation as Conf2. Thereby, four 4 × 4 MIMO combinations are constructed from the 6 × 6 measured positions for each location.

TABLE 2. System parameters from the IEEE802.15.3c standard for throughput evaluation.

Parameter	Value
Sampling rate	2640 MHz
FFT points	512
Number of subcarriers used for data	352
CP points	64
Modulation type	QPSK, 16QAM
Forward error correction	Structured LDPC
Coding rate	1/2

D. Physical Layer Specifications

We have applied the same parameters as are used in the IEEE 802.15.3c standard [13] since the parameters for the 94GHz band have not yet been defined. Table 2 gathers the physical layer specifications considered in this work. Simulations have been carried out for 16quadrature amplitude modulation (16QAM) and quadrature phase shift keying (QPSK) modulations and 1/2 coding rate. Interpolation has been used to derive the 512 frequency points described in the standard out of the 1024 reference points obtained in the laboratory, with a separation of 5.15 MHz between them. Besides, we simulate different STBC algorithms; specifically, orthogonal STBC (OSTBC) and quasi-orthogonal (QSTBC) architectures are analyzed for 4 × 4 MIMO system, whose rates are 1/2 and 1, respectively.

Table 3 indicates the physical layer bit rate (R_b) corresponding to each of the modulation and coding (MCS) and STBC schemes used.

TABLE 3. Bit rate for each modulation and coding scheme used.

MCS	Codingrate modulation	SISO / 4 × 4-QSTBC (Gbps)	4 × 4-OSTBC (Gbps)
1	1/2 QPSK	1.54	0.77
4	1/2 16QAM	3.08	1.54

III. CHANNEL CHARACTERIZATION

This section studies different parameters of the channel characterization using both vertical and horizontal polarization. We have used the configurations shown in Table 1 from the 6×6 array both to evaluate the throughput and to evaluate the correlation. However, in the SNR and Rician K factor evaluation we have averaged in each axial distance of the Tx/Rx antennas among the 180 possibilities (6×6×5), since in transmission and reception we use 6×6 uniform Rectangular array (6×6 URA) and Uniform Linear Array of 5 elements, respectively. Section III-A and III-B present the SNR and the Rician K factor, respectively. Lastly, Section III-C shows the transmission mean correlation.

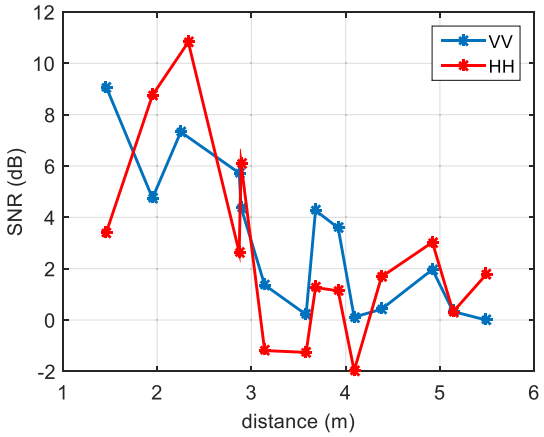

FIGURE 3. SNR (dB).

A. SNR

The SNR for both polarizations is shown in Fig. 3 computed as the average among the 512 frequencies. We first calculate the reference Equivalent Isotropically Radiated Power ($EIRP_{ref}$) from (1) to ensure that the lowest SNR (maximum distance for VV polarization) is 0 dB in the worst case. The algorithms used need a minimal SNR to function correctly. The noise level has been set at –78.8 dBm following the system model described in [16].

$$EIRP_{ref} = SNR_{\min} + L_{\max\_distance\_VV} - G_r + P_n \quad (1)$$

$$SNR = EIRP_{ref} - L + G_r - P_n \quad (2)$$

In (1), SNR_{min} is the minimal SNR, $L_{max\_distance\_VV}$ is the path loss to the maximum distance for VV polarization, G_r is the receiving antenna gain and P_n is the noise power.

Then we calculate the SNR existing at each distance by applying (2), where L is the path loss for each distance. The maximum EIRP according to the IEEE802.15.3c standard is 40 dBm [17] and in our system $EIRP_{ref}$ is equal to 10 dBm, being that such value is valid since it is below the maximum set by the standard.

B. RICIAN K FACTOR

It is also important to show the Rician K factor, extensively used in MIMO systems. If K is high indicates that the channel is more correlated and the capacity will decrease. It is defined

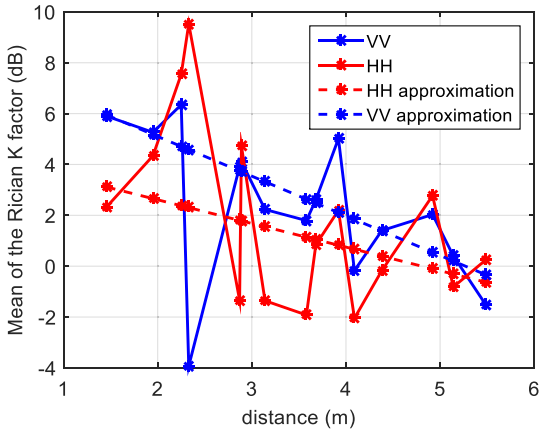

FIGURE 4. Mean of the Rician *K* parameter in dB: a) VV polarization. b) HH polarization.

as [18]:

$$K = \frac{\nu^2}{2\sigma^2} \tag{3}$$

which represents the ratio between power of the coherent LOS component and the power of the others scattered mutipath components (MPCs).

In Fig. 4, the mean of the Rician K parameter in dB, defined in (3), is plotted as a function of the Tx and Rx separation distance for the HH and VV polarizations. Generally speaking, the mean values of the K parameter are small ranging from -2.05 to 4.72 dB and from -1.74 to 6.26 dB for the HH and VV polarizations, respectively. Moreover, the mean of the K parameter tends to decrease as the Tx and Rx separation more pronounced for the VV polarization. To illustrate this effect, solid lines with the Mean Square Error (MSE) approximation have been depicted for both polarizations.

The K parameter values of the VV polarization are in general higher than the HH polarization values. This difference can be explained due to the position of the antennas. Vertical polarization implies omni propagation in the XY plane, while H polarization in the ZX plane. When measuring HH, depending on the difference in the Y dimension, the broadside directions are misaligned, thus leading to a lower K factor.

C. TRANSMISSION MEAN CORRELATION

Fig. 5a gives the variation of the mean correlation between the transmitting antenna elements using VV polarization for each antenna configuration and the mean correlation within the four configurations shown in Table 1. The correlation in reception is not shown because the same antenna configuration is always used. We obtain the correlation coefficients between the four transmitting antennas. Each correlation coefficient ($\rho_{p,q}$) between the transmitting antennas p and q for a given frequency f is calculated according the Kronecker model (4) [20]. The mean correlation between the transmitting antenna elements for each frecuency is computed as the average of those coefficient $\rho_{p,q}$. Finally, the correlation estimation is averaged over frequency bins (average among the 512 frequencies).

$$\rho_{pq}(f) = \frac{E\left[h^p(f) \cdot h^q(f)^*\right]}{\sqrt{E\left[|h^p(f)|^2\right] \cdot E\left[|h^q(f)|^2\right]}} \text{ with p } \neq \text{q.} \tag{4}$$

where E [] indicates the expectation operator and $h^p(f)$and $h^q(f)$ are the $p$and $q$columns of the channel matrix H(f) for a given frequency f, *respectively*. The channel matrix H(f) is defined as follows:

$$H(f) = \left(h^1(f)\, h^2(f)\, h^3(f)\, h^4(f)\right) \tag{5}$$

Where $h^i(f) = [h_1^i(f)\, h_2^i(f)\, h_3^i(f)\, h_4^i(f)]^{\mathrm{T}}$ is the column vector that represents the channel response in the frequency domain between the transmitting antenna i and each of the receiving antennas.

It shows that Conf1 has the worst correlation performance, but the rest of the configurations have similar trends to one another. Conf1 is perpendicular to the receiver array (see Table 1), so the elements are more correlated since all the energy is transmitted in the end-fire direction. Conf2 achieves the lowest correlation levels in certain distance intervals, for example, from 1.7 to 2.0 m and from 2.89 to 4.38 m. The system is highly correlated. For instance, the mean correlation is above 0.6 in most parts of the link for all of the configurations.

On the other hand, Fig. 5b shows the variation of the mean correlation between the transmitting antenna elements in the case of HH polarization. As in the VV case, a similar trend is observed for all of the configurations up to 4 m. Up to 2.33 m, it is observed that the correlation increases up to 0.9, but according to Fig. 3 the SNR improves for the HH case and exceeds 10 dB at that distance.

Comparing the SNR (Fig. 3) and the correlation (Fig. 5), the correlation has a trend which is proportional to the SNR −both for VV polarization and HH polarization− for 87% and 94% of the distances between Tx and Rx, respectively.

We can verify that the Rician K factor (Fig. 4) and the correlation (Fig. 5) also have a trend which is proportional for both VV and HH polarizations.

Finally, the relationship between the channel parameters can be explained as follows: if the K factor is increased, the portion of the Line Of Sight (LOS) signal is increased and the probability to encounter a deep fade decreases. Therefore, the LOS path becomes more significant and the fading is notably reduced. It explains that, usually, the correlation increases when factor K is greater and vice versa. For the same reason, if factor K is increased, the path loss decreases and hence the SNR increases.

IV. EVALUATION OF THE THROUGHPUT

This study focuses on the relation between different transmissions parameters, that is, the throughput, the transmitter configuration (according to Table 1), and the transmission distance. Furthermore, the throughput is obtained for distances ranging from 1.4 to 5.5 m.

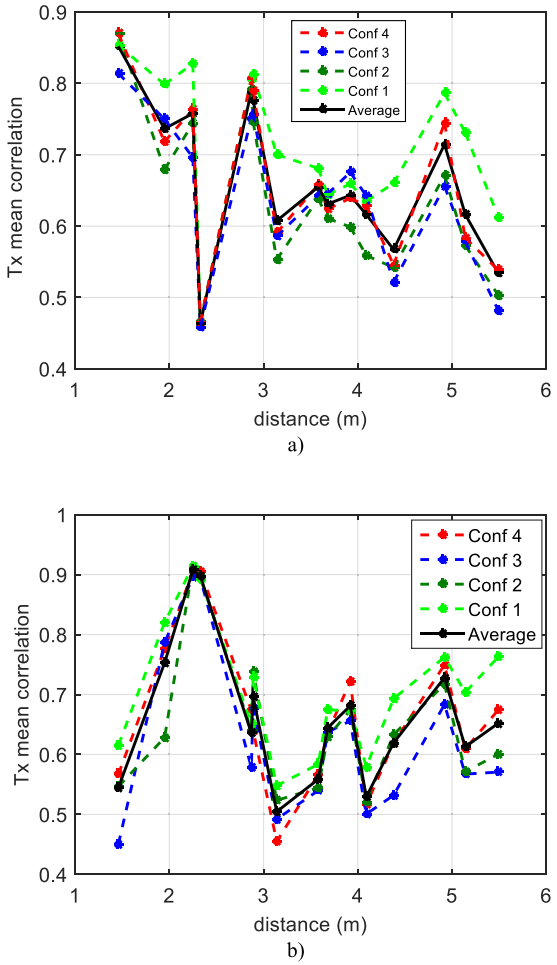

FIGURE 5. Mean transmitter correlation using: a) VV polarization. b) HH polarization.

First, the Packet Error Rate (PER) is obtained, and using the expression $Th = R_b(1 - PER)$, where R_b is the physical layer bit rate, we derive the throughput. We apply the Monte Carlo simulations and the statistics are computed from a software tool simulating the link, fully implemented in MATLAB, and by introducing 1000 transmitted packets. This leads to a minimum detectable PER $\leq 10^{-3}$, which is sufficiently low to compare the efficiency of these MIMO algorithms. To interpret the curves of the throughput that we show in Fig. 6, it is important to know that the PER depends on the SNR, on the MCS, and, of course, on the characteristics of the channel matrices.

A. PERFORMANCE FOR VV POLARIZATION

Fig. 6 shows the throughput performance corresponding to the MCS1 and MCS4 architectures. We focus on these cases to show the worst and the best cases. The gathered experimental data indicates that the throughput degrades sharply for schemes above MCS4 even at very short distances from the transmitter since it uses a higher-order modulation, and therefore upper schemes are not considered. The SISO case shows the throughput for MCS1, since, for MCS4, it is zero for all the distances. In addition, each MCS is simulated by

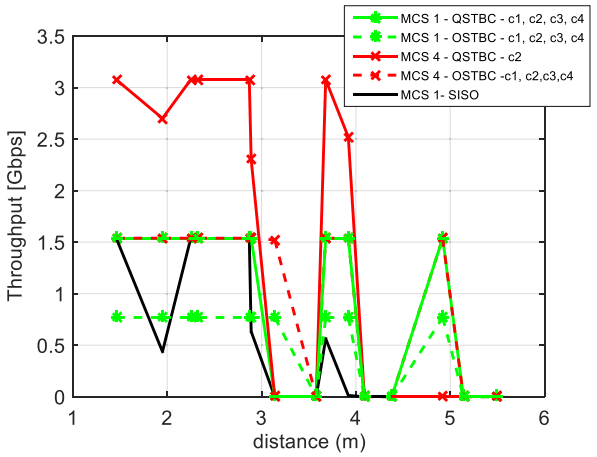

FIGURE 6. Best throughputs for SISO and MIMO (4,4) using either QSTBC or OSTBC architectures and MCS1 or MCS4 for VV polarization.

using both the QSTBC algorithm and the OSTBC, showing the best configurations for each case.

As QSTBC is not orthogonal, the chosen configuration of the antennas is very important [21], especially for the MCS4 case, since it uses a higher-order modulation and the high correlations have a great influence. As already outlined, Conf2 achieves the lowest correlation, offering the best performance. A maximum throughput of 3.08 Gb/s can be obtained using MCS4/QSTBC Conf2 at a distance below 2.87 m. To achieve this, the minimum SNR needed is 4.10 dB (see Table 4), since MCS4 uses a 16QAM modulation and up to this distance the mean correlation is 0.8, as shown the Fig. 5a. The maximum throughput achievable in the 2.87 to 3.14 m range is 1.54 Gb/s with MCS4/OSTBC and a minimum SNR of 1.30 dB, as shown in Table 4. Therefore, we observe that when using OSTBC algorithms, greater distances are achieved with lower SNR without influencing the correlation. The uneven behavior of the system throughput above a distance of 3.14 m does not guarantee a proper service. Nevertheless, in Fig. 3 we can observe that the SNR improves up to a level of 4 dB in the 3.6 – 4 m range. Therefore an improvement in throughput is observed in Fig. 6 at those distances.

The 2.87 and 3.14 m distances are the key to the interpretation of these results. The data gathered suggests that this is the maximum distance, regardless of the MCS/MIMO architectures. This is because, as shown in Fig. 3, the SNR level decreases to 4.3 dB in the 2.87 –3.14 m range and falls below 1 dB for distances greater than 3.14 m, except for the 3.6 – 4 m range mentioned before. We note that the SNR has a stronger effect on the throughput than the correlation; for example, in the range of 4.1 – 4.4 m the throughput decreases because the SNR decreases in this range, as shown in Fig. 3. However, Fig. 5a shows that the correlation decreases in this range, which should improve the throughput, but such improvement is not observed.

Finally, according to Fig. 6, the MCS4/QSTBC configuration performance exceeds that of SISO, considering that it achieves a greater throughput with a lower SNR.

TABLE 4. Best configuration, polarization, maximum Distance, and minimum SNR for each architecture.

MCS/ MIMO architecture	Best configuration	Polarization	Distance (m)	SNR (dB)
MCS4 QSTBC	Conf. 2	VV	2.87	4.10
	Conf. 3	HH	2.33	10.00
MCS4 OSTBC	Conf. 1, 2, 3,4	VV	3.14	1.30
		HH	2.87	2.10
MCS1 QSTBC	Conf. 1, 2, 3,4	VV	2.87	2.30
		HH		2.40
MCS1 OSTBC	Conf. 1, 2, 3,4	VV	3.14	1.20
		HH	2.87	1.60

B. COMPARING THE POLARIZATIONS: VV AND HH

Table 4 summarizes, for the best configurations, the maximum distance and the minimum SNR to achieve the throughout, both the vertical (VV) and horizontal (HH) polarization combinations. We note that it is better to use VV polarization than HH polarization. In all the MCS/MIMO architectures studied, the maximum achievable distance is obtained with the VV polarization with a lower level of SNR. This can be explained by the fact that, at both 2.87 and 3.14 m, the SNR is lower when applying HH polarization than when applying VV polarization, as shown in Fig. 3. Accordingly, in the MCS4 case whose modulation is 16QAM, applying HH polarization does not give the minimum SNR needed to achieve the same distance as that achieved using VV polarization. However, in the MCS1 case whose modulation is QPSK, even when QSTBC algorithms are used, a distance of 2.87 m can be reached both when HH polarization is applied and when VV polarization is applied. Finally, we observe in Table 4 that in the MCS4/QSTBC case using HH polarization, a minimum SNR of 10 dB is required to reach 2.33 m because the correlation is 0.89, as indicated in Fig. 5b.

V. CONCLUSION

To sum up, this work analyzes the experimental SNR and throughput data obtained for certain MCS/MIMO architectures in the 94 GHz band. The data gathered in the study indicates that this environment is highly correlated, with the average correlation exceeding 0.6 in most parts of the link. However, the throughput performance is influenced mainly by the SNR. Two polarization combinations have been simulated: VV polarization and HH polarization. It has been found that it is better to use VV polarization than HH polarization. In all the MCS/MIMO architectures studied, the maximum achievable distance is obtained with the VV polarization with a lower level of SNR. Thus, when using VV polarization and OSTBC algorithms, a distance of 3.14 m is reached, while with HH polarization the maximum distance is 2.87 m, since the experimental SNR is lower using HH polarization. Also, when applying a 4×4 QSTBC-MIMO architecture, the throughput is increased by a factor of four with respect to the SISO case. Finally, different antenna configurations have been simulated, noting that the configuration has a large impact on the performance, especially over large distances, in which case the SNR is so low that the throughput is zero.

REFERENCES

[1] European Project ICT-317669-METIS. (Apr. 2015). *Deliverable D8.4 METIS Final Project Report*. [Online]. Available: https://www.metis2020.com/documents/deliverables/

[2] V. Jungnickel *et al.*, "The role of small cells, coordinated multipoint, and massive MIMO in 5G," *IEEE Commun. Mag.*, vol. 52, no. 5, pp. 44–51, May 2014.

[3] T. S. Rappaport *et al.*, "Millimeter wave mobile communications for 5G cellular: It will work!" *IEEE Access*, vol. 1, pp. 335–349, 2013.

[4] K. Haneda, "Channel models and beamforming at millimeter-wave frequency bands," *IEICE Trans. Commun.*, vol. E98-B, no. 5, pp. 755–772, May 2015.

[5] T. S. Rappaport, E. Ben-Dor, J. N. Murdock, and Q. Yijun, "38 GHz and 60 GHz angle-dependent propagation for cellular & peer-to-peer wireless communications," in *Proc. IEEE Int. Conf. Commun. (ICC)*, Jun. 2012, pp. 4568–4573.

[6] T. S. Rappaport, G. R. MacCartney, M. K. Samimi, and S. Sun, "Wideband millimeter-wavepropagation measurements and channel models for future wireless communication system design," *IEEE Trans. Commun.*, vol. 63, no. 9, pp. 3029–3056, Sep. 2015.

[7] G. R. MacCartney, T. S. Rappaport, S. Sun, and S. Deng, "Indoor office wideband millimeter-wave propagation measurements and channel models at 28 GHz and 73 GHz for ultra-dense 5G wireless networks," *IEEE Access,* vol. 3, pp. 2388–2424, 2015.

[8] M. Sasaki, W. Yamada, T. Sugiyama, M. Mizoguchi, and T. Imai, "Path loss characteristics at 800MHz to 37 GHz in urban street microcell environment," in *Proc. 9th Eur. Conf. Antennas Propopag. (EuCAP)*, Lisbon, Portugal, Apr. 2015, pp. 1–5.

[9] S. Shou, M. Chung, C. T. Wu, Y. C. Chuang, and H.-C. Hsieh, "Preliminary design of 94 GHz E-band phase array antenna for future mobile communication," in *Proc. Asia–Pacific Int. Symp. Electromagn. Compat. Signal Integr. Tech. Exhibit. (APEMC)*, 2016, pp. 899–902.

[10] H. B. Yang, P. F. M. Smulders, and M. H. A. J. Herben, "Channel characteristics and transmission performance for various channel configurations at 60 GHz," *EURASIP J. Wireless Commun. Netw.*, vol. 1, Jan. 2007, Art. no. 19613.

[11] G. L. Stüber, J. R. Barry, S. W. McLaughlin, Y. Li, M. A. Ingram, and T. G. Pratt, "Broadband MIMO-OFDM wireless communications," *Proc. IEEE*, vol. 92, no. 2, pp. 271–294, Feb. 2004.

[12] X.-B. Liang, "A high-rate orthogonal space-time block code," *IEEE Commun. Lett.*, vol. 7, no. 5, pp. 222–223, May 2003.

[13] *Wireless Medium Access Control (MAC) and Physical Layer (PHY) Specifications for High Rate Wireless Personal Area Networks (WPANs) Amendment 2: Millimeter-Wave-Based Alternative Physical Layer Extension*, standard IEEE 802.15.3, 2009.

[14] *Wireless LAN Medium Access Control (MAC) and Physical Layer (PHY) Specifications Amendment 3: Enhancements for Very High Throughput in the 60 GHz*, standard 802.11ad, 2012.

[15] M.-T. Martinez-Ingles *et al.*, "Channel sounding and indoor radio channel characteristics in the W-band," *EURASIP J. Wireless Commun. Netw.*, vol. 30, p. 1, Jan. 2016, doi: 10.1186/s13638-016-0530-7.

[16] M. Kyro, K. Haneda, J. Simola, K. Takizawa, H. Hagiwara, and P. Vainikainen, "Statistical channel models for 60 GHz radio propagation in hospital environments," *IEEE Trans. Antennas Propag.*, vol. 60, no. 1, pp. 1569–1577, Mar. 2012.

[17] *ERC Recommandations 70-03*, accessed on Feb. 2017. [Online]. Available: http://www.erodocdb.dk/docs/doc98/official/pdf/rec7003e.pdf

[18] A. Abdi, C. Tepedelenlioglu, M. Kaveh, and G. Giannakis, "On the estimation of the K parameter for the Rice fading distribution," *IEEE Commun. Lett.*, vol. 5, no. 3, pp. 92–94, Mar. 2001.

[19] K. Sato *et al.*, "Measurements of reflection characteristics and refractive indices of interior construction materials in millimeter-wave bands," in *Proc. 45th IEEE Veh. Technol. Conf.*, Jan. 1995, pp. 449–453.

[20] D. P. McNamara, M. A. Beach, and P. N. Fletcher, "Spatial correlation in indoor MIMO channels," in *Proc. PIMRC* Sep. 2002, pp. 290–294.

[21] M. T. Martinez-Ingles *et al.*, "Experimental evaluation of an indoor MIMO-OFDM system at 60 GHz based on the IEEE802.15.3c standard," *IEEE Antennas Wireless Propag. Lett.*, vol. 12, pp. 1562–1565, 2013.

CONCEPCIÓN SANCHIS-BORRÁS was born in Valencia, Spain, in 1979. She received the Telecommunications Engineering degree from the Universidad Politécnica de Valencia, Spain, in 2004, and the Ph.D. degree in telecommunications from the Universidad Politécnica de Cartagena, Cartagena, Spain, in 2012. In 2006, she joined the Department of Technical Sciences, Universidad Católica San Antonio de Murcia, where she is currently an Associate Professor. Her current research interests include the signal processing techniques for MIMO and radio wave propagation.

MARÍA-TERESA MARTÍNEZ-INGLÉS was born in Murcia, Spain, in 1983. She received the Telecommunications Engineering degree and the Ph.D. degree in telecommunications from the Universidad Politécnica de Cartagena (UPCT), Cartagena, Spain, in 2009 and 2014, respectively. In 2016, she joined the University Center of Defense, San Javier Air Force Base, MDE-UPCT, Spain, where she is currently an Associate Professor. Her research line aims to study the modeling and characterization of the millimeter wave frequency band.

JOSÉ-MARÍA MOLINA-GARCÍA-PARDO received the Engineer of Telecommunications degree from the Universidad Politécnica de Valencia, Spain, in 2000, the M.Sc. degree in communication and signal processing in Newcastle upon Tyne, U.K., in 2001, and the Ph.D. degree in telecommunications from the Universidad Politécnica de Cartagena (UPCT), Spain, in 2004. In 2001, he joined the Information Technologies and Communications Department, UPCT, where he became an Associate Professor in 2007, and has been a Full Professor since 2016. He currently leads the SICOMO Research Group. He is also the Lead Researcher in some national projects, and participates actively in the European COST action IC-1004 (Radio Communications for Green Smart Environments). He has authored papers that have appeared in over 60 journals indexed in the JCR, over 100 international conferences, and three book chapters. His research activities are centered on radio-communications, propagation, channel modeling and experimental channel sounding in different frequency band (400MHz to 60GHz), and technologies (GSM, UMTS, LTE, WiFi, WSN, TETRA, mmW, OFDM, MIMO, and cognitive radio).

JUAN PASCUAL GARCÍA was born in Castellón, Spain, in 1975. He received the Telecommunications Engineering degree from the Technical University of Valencia, Valencia, Spain, in 2001, and the Ph.D. degree in communications engineering from the Universidad Politécnica de Cartagena (UPCT), Cartagena, Spain, in 2010. In 2003, he joined the Communications and Information Technologies Department, UPCT, as a Research Assistant and then became an Associate Professor. In 2009, he joined the SiCoMo Research Group, UPCT, where he is currently developing his research tasks. His current research interests include radio wave propagation, ray tracing techniques, and radio channel propagation models.

JOSÉ-VÍCTOR RODRÍGUEZ was born in Murcia, Spain, in 1975. He received the Telecommunications Engineering degree from the Universidad Politécnica de Valencia, Spain, in 2001, after doing his graduate thesis at the Lund Institute of Technology, Lund University, Sweden, in collaboration with Ericsson Mobile Communications AB, and the Ph.D. degree in communications engineering from the Universidad Politécnica de Cartagena (UPCT), Spain, in 2006. In 2002, he joined the Department of Information Technologies and Communications, UPCT, where he is currently an Associate Professor. His current research interests include the modeling of radio wave propagation in the mobile environment, with an emphasis on multiple-building diffraction.